ELSEVIER

International Journal of Mass Spectrometry 221 (2002) 245–262

International Journal of Mass Spectrometry

www.elsevier.com/locate/ijms

Dissociation of noncovalent protein complexes by triple quadrupole tandem mass spectrometry: comparison of Monte Carlo simulation and experiment

Victor J. Nesatyy [a,*], Julia Laskin [b]

[a] *Department of Chemistry, University of British Columbia, 2036 Main Mall, Vancouver, BC, Canada V6T 1Z1*
[b] *William R. Wiley Environmental Molecular Sciences Laboratory, Pacific Northwest National Laboratory, P.O. Box 999 (K8-96), Richland, WA 99352, USA*

Received 28 June 2002; accepted 4 October 2002

Abstract

We present Monte Carlo simulations of collisionally activated dissociation of noncovalent protein complexes in the collision cell of a triple quadrupole mass spectrometer. These simulations account for the influence of the precursor ion mass-to-charge ratio, acceleration potential, nature of the collision gas and the number of collisions experienced by the ion on the efficiency of ion dissociation. Evolution of the translational and internal energies of activated precursor ions along the collision cell was simulated using the hard-sphere and the diffuse scattering models. Dissociation rate constants and ion survival probability were calculated based on the estimated internal energy content of the excited ion. It was found that dissociation of the precursor ion could occur anywhere in the collision cell provided there is enough gain of relative internal energy accumulated during collisions. Simulated dissociation curves are in a good agreement with experimental results obtained for different collision gases at different pressures. Monte Carlo simulations of collision events modeled by the hard-sphere and diffuse scattering approximations resulted in different dynamics of precursor ion dissociation. Comparison of Monte Carlo simulations with results obtained using the previously proposed collision model showed a good correlation between the integral results obtained using these two approaches over a variety of experimental parameters. However, in contrast to the collision model, Monte Carlo simulations allow to obtain detailed information on the dynamics of ion dissociation in the collision cell. Moreover, Monte Carlo simulations provided a first insight into collisionally activated dissociation of the precursor ion under unfolding conditions including realistic increase in collision cross section during ion passage through the collision cell. (Int J Mass Spectrom 221 (2002) 245–262)

Keywords: Monte Carlo simulation; Triple quadrupole mass spectrometry; Collisional activated dissociation

1. Introduction

Application of electrospray ionization (ESI) allows transferring not only individual proteins but also multi-protein complexes from solution into vacuum [1–5]. Recent work in a number of laboratories utilized ESI–MS to estimate qualitatively and in some cases even quantitatively the affinity constants in solution [6,7]. Tandem mass spectrometry (MS/MS) experiments can provide valuable information on the gas-phase binding energies of protein complexes based on their dissociation [8].

* Corresponding author. Present address: EAWAG, AQU, Uberlandstrasse 133, CH-8600 Dubendorf, Switzerland.
E-mail: victor.nesati@eawag.ch

1387-3806/02/$ – see front matter
PII S1387-3806(02)01017-5

Binding energies of noncovalent protein complexes have been examined in the past using a variety of experimental approaches. Activation energies and pre-exponential factors were obtained using blackbody infrared radiative dissociation (BIRD) [9] and thermal dissociation of ions trapped in a Paul trap [10]. Although internal energy distributions of ions in thermal experiments are well defined, these experiments can be performed over a rather limited range of temperatures. Multiple-collision activation is a viable alternative to thermal dissociation studies. Collisionally activated dissociation of noncovalent protein complexes in triple quadrupole mass spectrometer has been studied either by increasing acceleration potential in the orifice-skimmer region of an electrospray interface [11] or by collisions with neutral gas inside the collision cell [12,13].

It is commonly assumed that low-energy collisional activated dissociation (CAD) is a two-step process, in which collisional activation/deactivation is followed by the unimolecular dissociation of excited ion [14,15]. A number of statistical approaches can be used to determine the rate of unimolecular dissociation [16,17]. However, significant difficulties remain in modeling internal energy deposited into the ion as a result of low-energy collisions. RRKM-based modeling has been developed to study the efficiency of energy transfer upon multiple collision activation of small peptide ions in the Penning trap [18–20]. It has been demonstrated that multiple-collision activation resulted in deposition of the same amount of internal energy into a series of protonated polyalanines [21]. This result was supported using master equation modeling. However, extending this approach to collisional activation of large protein complexes is not a trivial task. An additional complication of the studies involving triple quadrupole mass spectrometers is the scattering of ions during their passage through the collision cell.

Nevertheless, significant progress in characterization of the collision dynamics and deposition of internal energy into protein complexes during CAD process in triple quadrupole mass spectrometers has been achieved [22,23]. Tandem mass spectrometry experiments and collision model for an ion activation were used to measure the amount of internal energy accumulated by the ion in excess of its initial internal energy acquired in the ion source (relative internal energies), necessary to induce dissociation of complex gas-phase ions [24–26]. This model accounts for the translational energy loss of ions of different sizes and charge states, however, it does not provide an insight on the dynamics of ion dissociation during the passage of the precursor ion through the collision cell [24]. Simultaneous gain of internal energy and loss of translational energy of precursor ions occurring during multiple-collision activation is a typical stochastic problem. It is rather difficult to describe using analytical expressions but relatively easy to model using Monte Carlo simulation [23,27–29]. In this work CAD of Trypsin–BPTI complex ions inside collision cell of triple quadrupole mass spectrometer is modeled by Monte Carlo simulations based on the hard-sphere and the diffuse scattering models [22]. The effect of experimental parameters on the position of the survival probability curves modeled by Monte Carlo simulations is compared with previously published experimental data and predictions of the collision model [24].

2. Theory

2.1. Collision model for ion activation

Collisions of gas-phase molecules with an object can be described using diffuse or specular scattering models [30]. Diffuse scattering is characterized by a complete memory loss of the incident momentum and the particle leaves the object with a cosine distribution of angles perpendicular to the surface of the object [22]. In contrast, specular scattering is equivalent to the hard-sphere scattering and results in conservation of the component of the momentum parallel to the surface and reversal of the normal component [22]. Previous work showed that interaction of large protein ions and particles with collision gas is better described by the diffuse scattering model [31–33].

In MS/MS experiments in a triple quadrupole mass spectrometer, ions of protein complexes are injected into the collision cell with increasing energies. Relative internal energy, i.e., amount of internal energy accumulated by the precursor ion during its passage through the collision cell, ΔU, is proportional to the sum of the center-of-mass collision energies for each of a series of low-energy collisions and is given by [26]

$$\Delta U = \frac{m_2}{M}\mathrm{TR}_0\frac{m_1}{m_2}\frac{\phi}{C_\mathrm{D}}\left[1-\exp\left(-\frac{C_\mathrm{D}nm_2\sigma l}{m_1}\right)\right] \quad (1)$$

where m_1 and m_2 are masses of the ion and the collision gas, respectively, $M = m_1 + m_2$, n the number density of the collision gas, l the distance traveled by the ion, C_D a drag coefficient [30–32], σ the collision cross-section, ϕ the average fraction of the center-of-mass collision energy transferred into the internal energy of the ion in collision and TR_0 is the initial translational energy of the ion injected into the collision cell.

The only unknown parameter in this equation is the conversion efficiency of the center-of-mass collision energy into the internal energy, ϕ. However, there is an increasing body of evidence suggesting that the energy transfer efficiency increases with the size of the ion reaching 90% for a nonapeptide [34,35]. It is reasonable to assume that even higher energy transfer efficiency reaching 100% would be characteristic of collisions of larger ions, such as protein complexes, with light collision gas [25].

2.2. Monte Carlo simulation

Two Monte Carlo models were developed to simulate the translational energy loss for ions passing through the collision cell uniformly filled with a gas. The simple model assumes 100% energy transfer efficiency and the average scattering angle of 90°, characteristic for hard-sphere collisions. The second model, further referred to as the diffuse model, simulates ion motion through a collision cell taking into account statistically generated distribution of scattering angles and energy transfer efficiencies.

2.2.1. The simple model

To illustrate the principle of the method, the algorithm of the simple model is briefly described here. Consider an ensemble of ions with initial internal energy U_0 entering the collision cell. The initial translational energy (TR_0) of the ions is determined by their charge state and the acceleration potential. Monte Carlo simulations model the motion of ions in the collision cell by statistically calculating distances between collisions traveled by each ion until the total distance equals the length of the collision cell. The probability of an ion to experience a collision (ξ) at a distance l in the collision cell with gas number density n is given by

$$\xi(l) = 1 - \exp(-\sigma nl) \quad (2)$$

where σ is the collision cross-section.

Collision probabilities, ξ, were statistically generated and distances traveled by the ion between collisions were determined by

$$l_i = -\frac{\ln(1-\xi_i)}{n\sigma} \quad (3)$$

where $i \geq 1$ is the collision number.

Having traveled the distance l_i the ion with translational energy TR_{i-1} was considered to experience an ith collision. The ratio of the ion kinetic energy before and after collision is given by [22]

$$\frac{\mathrm{TR}_i}{\mathrm{TR}_{i-1}} = \frac{m_1^2+m_2^2}{M^2} - \frac{m_2U_i}{M(\mathrm{TR}_{i-1})} + \frac{2m_1m_2}{M^2}\sqrt{1-\frac{U_iM}{m_2(\mathrm{TR}_{i-1})}}\cos\theta_\mathrm{CM} \quad (4)$$

For inelastic collisions the amount of translational energy transferred into the internal energy is given by $\Delta U_i = \phi(m_2/M)\mathrm{TR}_{i-1}$. The simple Monte Carlo model assumes the average fraction of the transferred energy of 1, thus neglecting variation of the average scattering angle which was considered to be 90° in the collision model for an ion activation. Thus, the amount of lab energy retained by the ion after ith collision is

given by a simple expression:

$$\mathrm{TR}_i = \mathrm{TR}_{i-1}\left(\frac{m_1^2}{M^2}\right) \tag{5}$$

The time between collisions is then given by

$$t_i = \frac{l_i}{(2\mathrm{TR}_i/m_1)^{1/2}} \tag{6}$$

The gain in the internal energy following collision is equal to the center-of-mass energy ($(m_2/M)\mathrm{TR}_{i-1}$). The amount of internal energy accumulated after ith collision is given by

$$U_i = U_{i-1} + \left(\frac{m_2}{M}\right)\mathrm{TR}_{i-1} \tag{7}$$

The dissociation rate constant was calculated using the RRKM expression:

$$k_i = \nu\left(\frac{U_i - E_0}{U_i}\right)^s \tag{8}$$

where ν is the frequency factor, E_0 the dissociation threshold and s is the number of vibrational degrees of freedom of the excited ion.

The survival probability of the precursor ion between successive collisions is given by

$$P_i = \exp(-k_i t_i) \tag{9}$$

The total distance traveled by the ion between collisions (L_i) was calculated and iterations were repeated for a number of collisions (w), necessary to travel through the entire length of the collision cell (20 cm).

The survival probability of the ion after j collisions ($1 \le j \le w$) at a distance L_j from the cell entrance can be estimated using the following expression:

$$P(L_j) = \prod_{i=1}^{j} P_i \tag{10}$$

For a given acceleration potential the average dissociation rate constant and internal energy accumulated during collisions can be determined from:

$$\langle k\rangle = \frac{\sum_{i=1}^{w} k_i(1-P_i)\prod_{i=1}^{w}P_i}{\sum_{i=1}^{w}(1-P_i)\prod_{i=1}^{w}P_i},$$

$$\langle U\rangle = \frac{\sum_{i=1}^{w} U_i(1-P_i)\prod_{i=1}^{w}P_i}{\sum_{i=1}^{w}(1-P_i)\prod_{i=1}^{w}P_i} \tag{11}$$

The average total distance traveled by ion between collisions is given by

$$\langle L\rangle = \frac{\sum_{i=1}^{w}[L_i + (l_{i+1} - l_i)/2](1-P_i)}{\sum_{i=1}^{w}(1-P_i)} \tag{12}$$

The average rate constant, internal energy and distance in the cell at which dissociation occurs can be estimated from the 50% cumulative survival probability. The entire calculation is then repeated several times and the results are averaged. The number of iterations was 13 in this study. Additional increase in the number of iterations did not result in a significant improvement in reproducibility. Plots of cumulative survival probabilities at the cell exit as a function of the acceleration voltage are constructed and compared with experimental results.

2.2.2. The diffuse model

Monte Carlo simulations based on the diffuse scattering model use the same algorithm while correcting for the average scattering angle and the average fraction of the transferred energy. In the diffuse model, the average fraction of the transferred energy, ϕ, is less then 1, and the average scattering angle can be varied from 0 to 180°. Thus, the ratio of the ion kinetic energy before and after collision is given by

$$\frac{\mathrm{TR}_i}{\mathrm{TR}_{i-1}} = \frac{m_1^2 + m_2^2}{M^2} - \frac{\phi m_2^2}{M^2} + \frac{2m_1m_2}{M^2}\sqrt{1-\phi}\cos\theta_{\mathrm{CM}} \tag{13}$$

The amount of internal energy accumulated after ith collision is given by

$$U_i = U_{i-1} + \phi\left(\frac{m_2}{M}\right)\mathrm{TR}_{i-1} \tag{14}$$

Histograms of the average fraction of the energy transfer efficiencies and scattering angles are shown in Fig. 1. Distribution of scattering angles was calculated from the statistically generated impact parameter of the collision as described previously [23]. Average value of the statistically generated scattering angle was 136°, which is in agreement with previous studies [22]. The distribution of energy transfer efficiencies

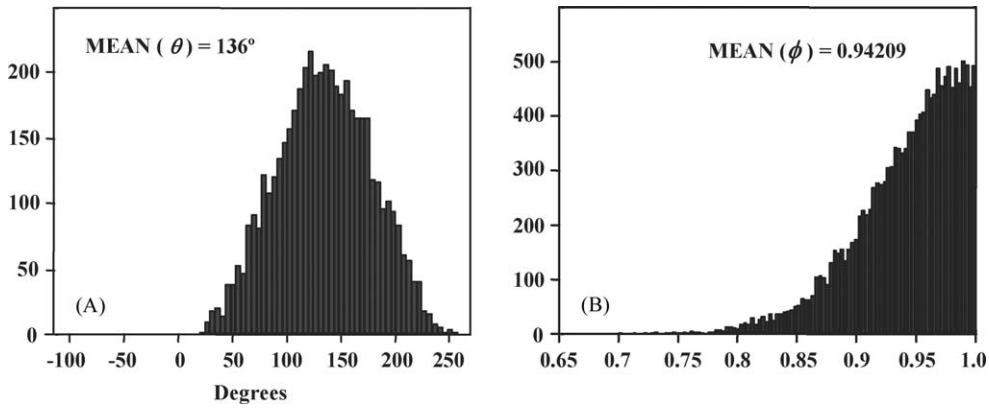

Fig. 1. Typical computer generated distribution of (A) scattering angles, (B) average fraction of center-of-mass energy transferred to internal energy, that were used in Monte Carlo simulation based on the diffuse scattering model.

with a mean of ∼0.94 was arbitrarily constrained to the range from 0.7 to 1.

3. Results and discussion

3.1. Single ion simulations

The results of the simple model simulation of the motion of a single ion (MW = 30,000; charge state: +12) through the collision cell uniformly filled with 0.5 mTorr of Kr are shown in Fig. 2. In this simulation RRKM parameters were chosen rather arbitrarily. The collision cross section of 2000 Å^2 was estimated based on the suggested collision cross sections of protein complexes of similar molecular weight [24].

The number of collisions experienced by the ion increases linearly along the length of the collision cell uniformly filled with neutral gas (Fig. 2A). The increase in the number of collisions is accompanied by a gradual increase in the internal energy accumulated by the ion as it moves through the collision cell (Fig. 2B). The increase in the internal energy is faster for ions having a higher initial kinetic energy. It should be noted that the internal excitation of the precursor ion is not a linear function of its position along the collision cell. Loss of the translational energy following collision leads to a decrease in the center-of-mass collision energy, responsible for ion excitation, and the much slower internal energy build-up towards the exit from the collision cell.

Relatively slow increase in the internal energy results in almost exponential growth in dissociation rate constants (Fig. 2C). Obviously, ions that have lower initial kinetic energy will remain intact at the cell exit, while higher-energy ions will fully decompose before they exit the cell. Fig. 2D shows the cumulative product of survival probabilities for precursor ions at each point in the collision cell for a number of acceleration potentials. In this case dissociation of the precursor ion occurs closer to the cell end. However, for higher acceleration voltage dissociation occurs at shorter distances. Product of survival probabilities at each point of the collision cell gives the total survival probability at the cell exit. This simulation was repeated for a number of acceleration potentials from 10 to 250 V and the resulting fragmentation efficiency curve is shown in Fig. 2E. The shape of the simulated dissociation curve closely resembles the experimental dissociation curves reported in the literature [24,25]. Reproducibility of these simulations was significantly improved by increasing the ion population to 700 ions, which was used throughout this work.

Our results are qualitatively consistent with the results obtained previously using a simplified modeling approach, indicated that, unless ions accumulate

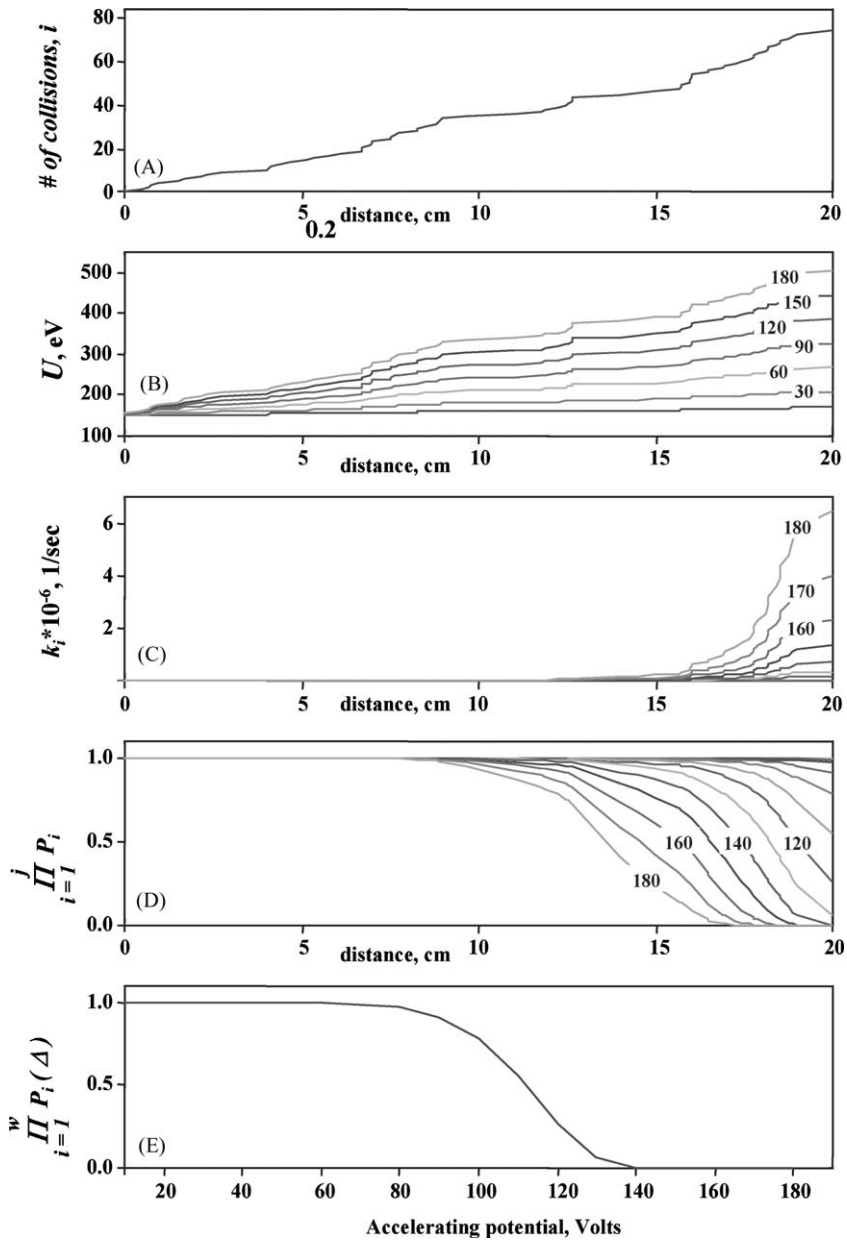

Fig. 2. Monte Carlo simulation of the single ion passing through collision cell. Plots of (A) number of collision, (B) internal energy, (C) dissociation rate constant, (D) cumulative survival probabilities along the collision cell, and (E) dissociation of precursor ion vs. acceleration potential (Δ). Mass of the precursor ion 30,000, charge state +12, collision cross section (σ) 2000 Å^2, initial internal energy (U_0) 150 eV, dissociation threshold (E_0) 1 eV, number degrees of freedom (s) 6000, frequency factor (ν) 10^{12} s^{-1}, collision gas Kr, pressure 0.5 mTorr. Numbers inside panels B, C, and D indicate acceleration potentials.

sufficient internal energy in the ion source, dissociation of the precursor ion mostly takes place in the last 4–5 cm of the collision cell [25]. It should be noted that simulated dissociation distance depends on a number of parameters (injection energy, the number density and the mass of the collision gas). Moreover, we found that variations in RRKM parameters such as the frequency factor, threshold energy and numbers of effective oscillators also have a strong effect on the distance traveled by the precursor ion prior to its simulated dissociation. Presented Monte Carlo simulation showed that dissociation could occur in *any* part of the collision cell, depending on the RRKM parameters. Specifically, under similar activation conditions ions with a smaller number of vibrational degrees of freedom and lower binding energies fragment close to the entrance into the collision cell, while larger and more tightly bound complexes dissociate closer to the cell exit.

3.2. Comparison of Monte Carlo simulations based on a simple and diffuse collision models

Previous reports on the calculation of collision cross section of protein ions showed that analysis of the results using diffuse collision model showed better correlation with known theoretical values [32,33]. Now it will be of interest to see whether use of either simple or diffuse collision model during the Monte Carlo simulation will result in significant differences of CAD. Results of Monte Carlo simulations obtained using the simple and the diffuse collision model are compared in Fig. 3. Left panels of Fig. 3 show plots of cumulative survival probability, rate constant and relative internal energy accumulated by the precursor ion moving along the collision cell calculated using these two models. Right panels of Fig. 3 show the dependence of total survival probability, rate constant and average internal energy accumulated by the precursor ion at the exit from the collision cell on the acceleration potential.

According to the diffuse model the amount of internal energy necessary for dissociation of the precursor ion is reached at a longer distance as compared to the simulation based on the simple collision model (Fig. 3B). Relatively small differences in the values of accumulated internal energies obtained from diffuse and simple models resulted in a considerable, almost two times, difference in the values of dissociation rate constants at the exit from the collision cell. Obviously, the increase in the dissociation rate constant is slower for the diffuse model (Fig. 3C) and the survival probability is shifted towards the cell exit (Fig. 3A). Differences in relative internal energies required for dissociation obtained from the two models result from the different distribution of scattering angles and the assumption of a lower efficiency of energy transfer in the diffuse model ($\langle\phi\rangle = 0.942$) as compared to the simple model ($\phi = 1$). The average internal energy increases gradually with increase in the acceleration voltage reaching a plateau at higher acceleration potentials (Fig. 3E). For both models plots of the average rate constant vs. the acceleration potential (Fig. 3F) have a sigmoidal shape. However, as discussed earlier the diffuse model predicts consistently lower values for average rate constants than the simple model.

3.3. Simulation of collisionally activated dissociation under unfolding conditions

It has been mentioned earlier that calculations of relative internal energy using Monte Carlo simulation and the collision model for ion activation do not account for variations in the size of the precursor ion. It is likely that increase in the internal energy of the precursor ion during its motion through the collision cell can result in unfolding of the ion and increase in its collision cross section. We investigated the effect of the increase in collision cross section of the precursor ion passing through the collision cell using the simple model Monte Carlo simulations. It was assumed that the collision cross section of the precursor ion increases gradually along the collision cell with the overall increase of 50%. The results obtained with and without unfolding are compared in Fig. 4. Since the collision cross section of the ion that undergoes unfolding during its flight through the collision cell increases, the number of collisions experienced by the ion increases correspondingly (Fig. 4A). This results in a steeper increase in the internal energy (Fig. 4B) and the dissociation

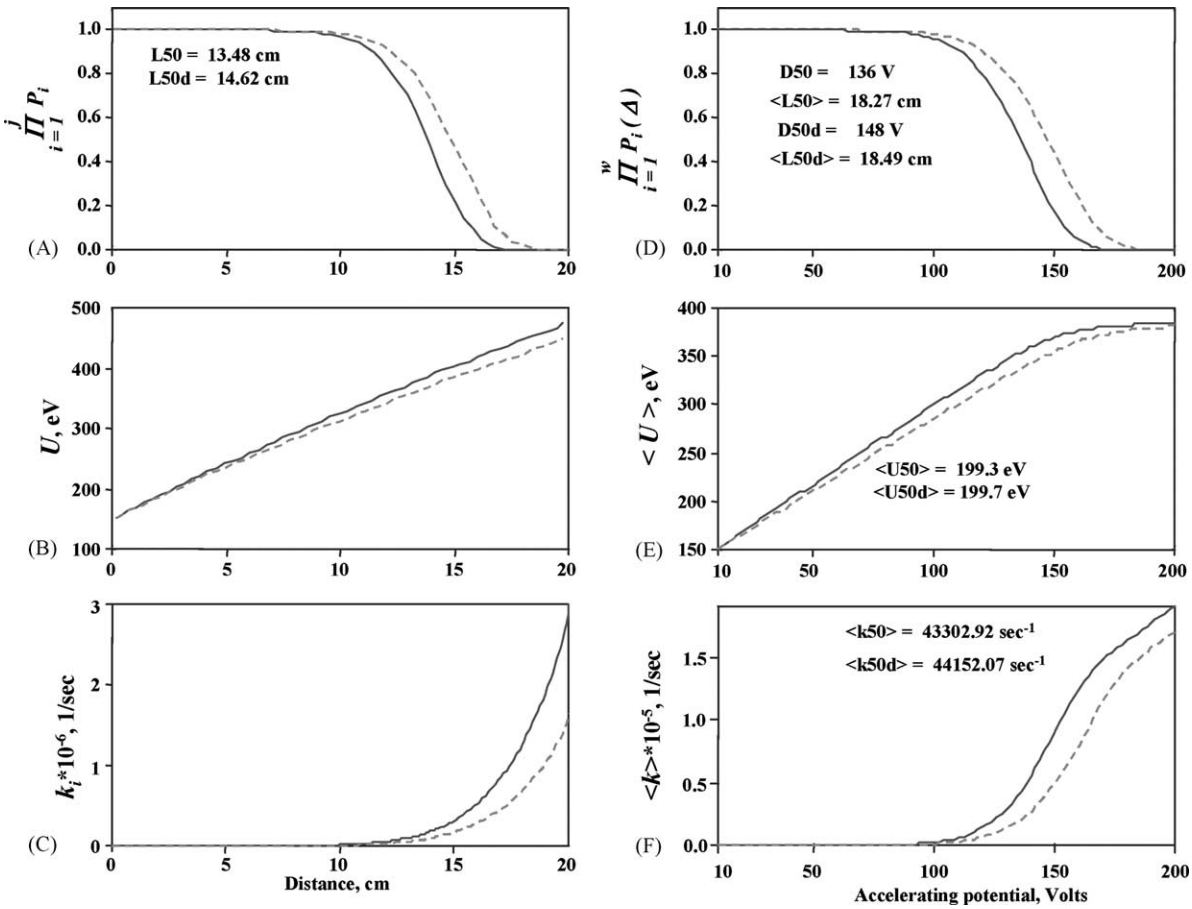

Fig. 3. Comparison of Monte Carlo simulation based on a simple and diffuse scattering collision models. Panels A, B, and C are respective plots of survival probability, internal energy, and rate constant along the collision cell at 200 V acceleration potential. Panels D, E, and F are plots of product of survival probabilities, average internal energy, and average rate constant at different acceleration potentials. Simulation parameters are the same as in Fig. 2. Solid and dashed lines correspond to results from simple and diffuse Monte Carlo simulation, respectively.

rate constant (Fig. 4C). Consequently, dissociation of the unfolded ion occurs further away from the cell exit (Fig. 4D) and the resulting dissociation curve (Fig. 4E) is shifted towards lower acceleration voltages. Comparable increase in the relative internal energy under similar experimental conditions was obtained using the collision model and assuming that in Eq. (1), the collision cross section of the precursor ion increases by $\Delta\sigma$ at distance increments of Δz. In the above simulation it was assumed that dissociation parameters for folded and unfolded ions are the same. A more realistic approach should take into account changes in stability of different conformations commonly observed in ion mobility experiments [36,37]. In conclusion, two-time increase in the collision cross section of an unfolding ion affected its dissociation kinetics to the much lesser extent then proportional changes in the mass of the collision gas and its number density.

3.4. Comparison with experimental data

In this section dissociation curves, dissociation voltages (acceleration voltage corresponding to 50% fragmentation of the precursor ion) and relative internal

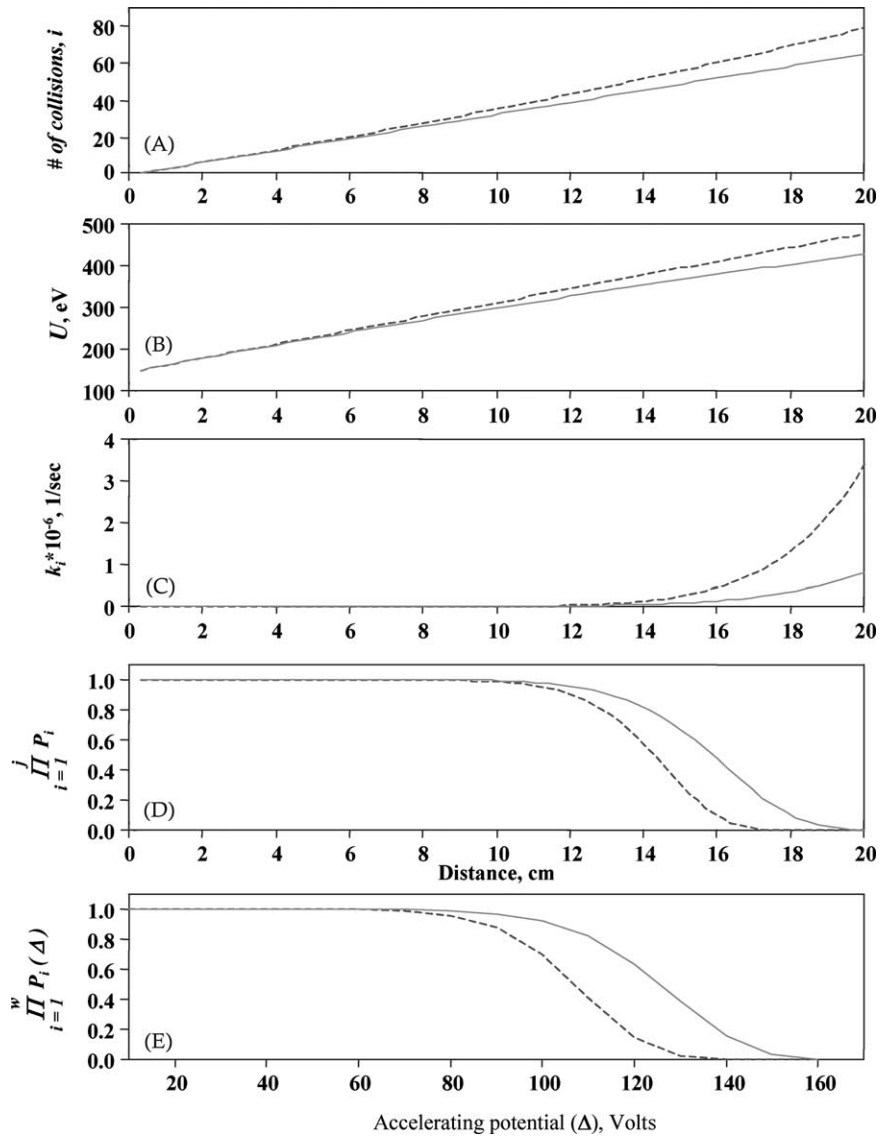

Fig. 4. Monte Carlo simulation of the unfolding ion passing through the collision cell. Plots of (A) number of collision, (B) internal energy, (C) dissociation rate constant, (D) cumulative survival probabilities along collision cell length, and (E) dissociation of precursor ion vs. acceleration potential (Δ). Simulation parameters are the same as in Fig. 2. Collision cross section (σ) are either constant 2000 Å^2 (solid line), or gradually increasing from 2000 to 3000 Å^2 (dashed line).

energies obtained using Monte Carlo simulations are compared with experimental data for +12 and +13 charge states of Trypsin–BPTI complex reported elsewhere [24].

Dissociation parameters for the RRKM equation during Monte Carlo simulations were determined by fitting shape and dissociation voltage of modeled dissociation curve to the experimental dissociation curve for the +12 charge state of the Trypsin–BPTI complex obtained for collisions with Kr at 0.5 mTorr, chosen as a reference point for both simple and diffuse Monte Carlo models. These parameters remained the

same for other pressures and collision gases. The effective number of oscillators (s in Eq. (8)) was chosen to be equal to one-half of the total number of vibrational degrees of freedom of the complex as suggested elsewhere [16], i.e., 3140 for the +12 charge state of Trypsin–BPTI complex consisting of 2095 atoms and 3141 for the +13 charge state. Best fit of diffuse Monte Carlo simulations with experimental data for the +12 charge state was achieved by adjusting the initial internal energy of the precursor ion (U_0) to 35 eV, threshold energy (E_0) to 0.4 eV, reaction frequency to $5 \times 10^7\ s^{-1}$. Monte Carlo simulations based on the simple collision model used the same set of RRKM parameters, except for U_0, which was adjusted to 25 eV for the +12 charge state to obtain a good fit with experimental data. It should be noted that evaluation of dissociation rate constants of the precursor ion using RRKM expression is simplistic. It is used here as a first approximation for semi-quantitative comparison with experimental data and is not intended to be utilized for detailed characterization of the dissociation energetics of a particular noncovalent protein complex.

Initially, the same set of RRKM parameters was used in the simulation conducted for both +12 and +13 charge states. However, dissociation voltages for the +13 charge state obtained using the same RRKM parameters show a rather poor correlation with experimental data. We found a substantially better agreement between experimental and simulated results by increasing the initial internal energy of the +13 charge state to 41 and 49 eV for simple and diffuse Monte Carlo simulations, respectively. A higher level of internal excitation accumulated by the +13 charge state in the ion source can be easily rationalized by the higher kinetic energy accumulated by this ion in the presence of acceleration fields. This results in more energetic collisions of the +13 charge state in the ESI interface and a more efficient heating of this ion as compared to the +12 charge state. The experimental data for the +13 charge state could be also reproduced by keeping the initial internal energy the same as for the +12 charge state and varying the threshold energy.

3.4.1. Effect of charge state on the dissociation of precursor ion

3.4.1.1. Comparison of simulated and experimental dissociation voltages. The results of Monte Carlo simulations for dissociation voltages obtained at five different pressures of three collision gases using diffuse model are summarized in Table 1. Very similar values were obtained using the simple model Monte Carlo simulations (data not shown). Results presented in Table 1 show that dissociation voltage of the precursor ion is affected by its charge state. Fig. 5A shows that the dissociation curve for the +13 charge state is shifted towards lower acceleration voltages. Experimental data shown in Table 1 indicates that addition of a proton to the +12 charge state of the Trypsin–BPTI complex results in decrease of the D_{50} from 114.5 to 90.6 V. Similar trend was observed in Monte Carlo simulations (Fig. 5A). The shift in dissociation curve as a function of the charge state (Fig. 5A) can be attributed to the increase in the initial kinetic energy following increase in the charge state. The initial kinetic energies for both charge states resulting in 50% fragmentation of the precursor ion are shown in Fig. 5B. Obviously, dissociation of the +13 charge state occurs at lower initial kinetic energy. However, the differences in kinetic energies are rather small (<15%). The lower kinetic energy required for ion dissociation can be either attributed to a lower stability of the +13 charge state of the complex or to the higher initial excitation of the +13 charge state acquired in the ion source.

3.4.1.2. Comparison of experimental and simulated relative internal energies. Relative internal energy (RIE) is the internal energy in excess of the initial internal excitation of the ion (acquired in the ion source) required to observe dissociation in the collision cell. Initial ion excitation strongly depends on source conditions. For example, different charge states of the same protein complex are excited differently in the orifice-skimmer region of the source. We use RIE for comparison with experimental data because the position of experimental dissociation curves reflects the

Table 1
Experimental and computer generated parameters of dissociation for gas-phase ions of Trypsin–BPTI noncovalent complex at different pressures of collision gases

Gas	P (mTorr)	Experimental		Diffuse Monte Carlo model			
		Dissociation voltages (V)		Dissociation voltages (V)		Reaction time (μs)	
		+12	+13	+12 ($U_0 = 35$ eV)	+13 ($U_0 = 49$ eV)	+12 ($U_0 = 35$ eV)	+13 ($U_0 = 49$ eV)
Ne	1.0	151	120	132	102	67	74
	1.2	129	102	108	86	76	82
	1.4	114	90	94	73	83	90
	1.6	102	81	83	65	89	98
	1.8	91	72	74	58	96	104
Ar	0.4	160	134	166	126	59	67
	0.5	124	99	133	103	67	74
	0.6	109	86	109	86	76	83
	0.8	86	68	84	65	89	97
	1.0	68	54	68	53	102	111
Kr	0.2	143	115	159	127	60	65
	0.25	119	89	127	98	69	77
	0.3	99	76	105	82	77	85
	0.4	77	60	80	63	92	99
	0.5	66	50	65	51	104	114

RIE for dissociation rather than the absolute internal energy of the excited ion. In order to extract the absolute value of internal excitation from experimental data the initial excitation of ions in the ion source must be carefully controlled.

RIE required to observe 50% fragmentation of the precursor ion were calculated using both the collision model (Eq. (1)) and Monte Carlo simulations. The collision model data was obtained directly from the experimental values of dissociation voltages (D_{50}).

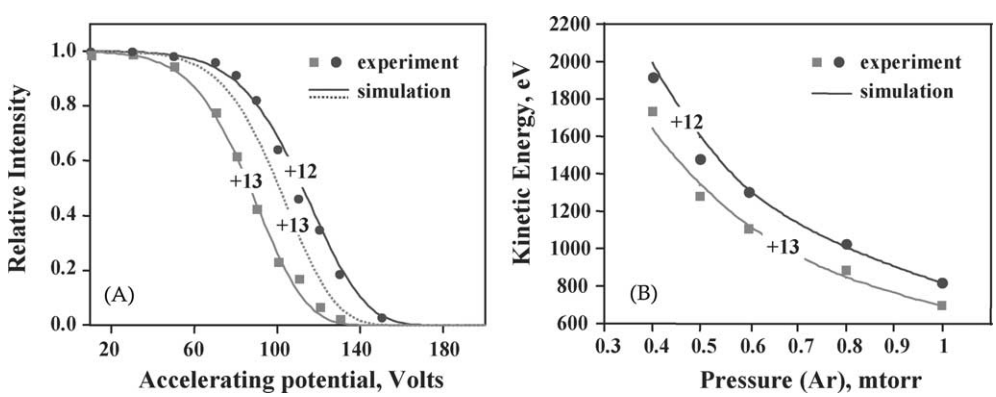

Fig. 5. Effect of the charge state on the dissociation of Trypsin–BPTI complex. Symbols represent experimental data, while solid lines correspond to simulation. Mass of the precursor ion 29,834, collision cross sections (σ) are 1866 and 1928 Å^2, for the +12 and +13 charge states, respectively. Panel A shows results of Monte Carlo simulation fitted to experimental data at 0.6 mTorr of Ar. For Monte Carlo simulation of +13 charge state, solid and dashed lines correspond to data obtained with initial internal energies U_0 of 49 and 35 eV, respectively. Panel B shows comparison of simulated and experimental values of initial kinetic energy required to dissociate precursor ion at different Ar pressures.

Table 2
Experimental and simulated values of relative internal energies required to dissociated gas-phase ions of Trypsin–BPTI noncovalent complexes

Gas	P (mTorr)	Relative internal energy (eV)					
		Collision model		Diffuse Monte Carlo model		Simple Monte Carlo model	
		+12	+13	+12 ($U_0 = 35$ eV)	+13 ($U_0 = 49$ eV)	+12 ($U_0 = 25$ eV)	+13 ($U_0 = 41$ eV)
Ne	1.0	135	120	132	114	143	123
	1.2	136	120	129	112	140	121
	1.4	138	122	127	109	139	118
	1.6	139	122	125	107	136	117
	1.8	137	120	123	106	134	115
Ar	0.4	116	108	135	116	146	127
	0.5	110	98	132	114	143	124
	0.6	114	100	129	111	141	121
	0.8	115	102	125	107	137	117
	1.0	110	97	122	104	133	113
Kr	0.2	108	96	134	117	146	126
	0.25	110	92	131	113	143	123
	0.3	107	91	128	110	140	121
	0.4	108	94	124	107	136	117
	0.5	110	93	120	104	133	113

Both simple and diffuse model Monte Carlo simulations were referenced to the same experimental point (collisions with Kr at 0.5 mTorr) as described earlier. The results are summarized in Table 2.

Assuming the same initial internal energy for both charge states, very similar values of RIE were generated by diffuse Monte Carlo simulations (data not shown). Similar results were produced for simple Monte Carlo simulations. Increase in the initial internal energy resulted in somewhat lower values of RIE for the +13 charge state. This is not surprising because RIE are referenced to the initial internal energy, U_0, of the ion, which is different for the two charge states. Namely, for the +12 charge state RIE generated during diffuse Monte Carlo simulations refers to the internal energy in excess of 35 eV, while for the +13 charge state RIE is the internal energy in excess of 49 eV. After accounting for 14 eV difference in the initial excitation for the +13 charge state there remains only 3% difference between internal energies required to observe dissociation for the two charge states. This suggests that dissociation parameters for both charge states of the Trypsin–BPTI complexes are very similar. However, because it is impossible to distinguish between the internal excitation gained by ions in the ion source and in the collision cell, quantitative comparison between the reactivity of different charge states can be achieved only by carefully controlling the initial excitation of different charge states of the precursor ion.

The dependence of dissociation energetics of protein complexes on the charge state has been debated in the literature. Activation energies of the +9 and +12 charge states of the heme–protein complex electrosprayed from pseudo-native solution measured in BIRD experiments are very similar [9]. However, the same complex electrosprayed from denaturing solution demonstrated decrease in activation energies with increase in the charge state [9]. The differences in the dissociation energetics of these complexes were rationalized by different solution conformations of the ions [9]. In contrast, similar values of activation energies for the +8 to +20 charge states of unfolded heme–protein complex were found in CAD trapping experiments [26]. However, studies of the gas-phase binding of the heme–protein complex by

tandem mass spectrometry showed that similar values of relative internal energies were obtained only for charge states ranging from +10 to +14 [26]. Further increase in charge states from +15 to +19 resulted in a consistent decrease of relative internal energies. This is consistent with recent observation by Chen and coworkers showing the same phenomenon [25].

3.4.2. Effect of the collision gas nature and its pressure on the dissociation of precursor ion

3.4.2.1. Comparison of simulated and experimental dissociation voltages. The nature and the number density of the collision gas have a strong effect on the collisionally activated dissociation of ions in the collision cell. Fig. 6 shows that dissociation voltage, D_{50}, decreases with increase in the mass and the number density of the collision gas. Increase in the mass of the collision gas results in the corresponding increase in the center-of-mass collision energy available for ion excitation and a faster accumulation of the internal energy required observing fragmentation. It follows that dissociation voltage should show a linear dependence on the mass of the collision gas. Obviously, increasing the number density of the collision gas increases the number of activating collisions and results is a faster excitation of the precursor ion.

Analysis of the experimental data for +12 and +13 charge state of Trypsin–BPTI complexes showed that the dissociation voltage obtained for 1 mTorr of Ar (68.5 and 54.1 V) were twice as small as dissociation voltages obtained for 1 mTorr of Ne (150.9 and 119.6 V). Two-fold increase in the MW of the collision gas resulted in the decrease in the values of D_{50} by a factor of 2.2 (Table 1). Similar results were observed during Monte Carlo simulations of the dissociation of this complex with different collision gases of the same pressure (Fig. 6A). For both charge states dissociation voltage obtained with 1 mTorr of Ne was almost two times higher than the voltage obtained with 1 mTorr of Ar (Table 1).

Simulations of halfway dissociation voltages by both simple and diffuse Monte Carlo model show a good agreement with experimental data for both +12 and +13 charge states (Fig. 6) with Ar and Kr as collision gases. The deviation between the experimental and calculated results is less than 10% for all pressures. However, calculated dissociation voltages for collisions with Ne are systematically underestimated by 20–25%. The differences between the results obtained for Ne can be rationalized assuming that conversion of the center-of-mass collision energy into the internal excitation of the precursor ion is less efficient for Ne than for Ar and Kr. In fact, excellent agreement between experimental results and simulation for collision

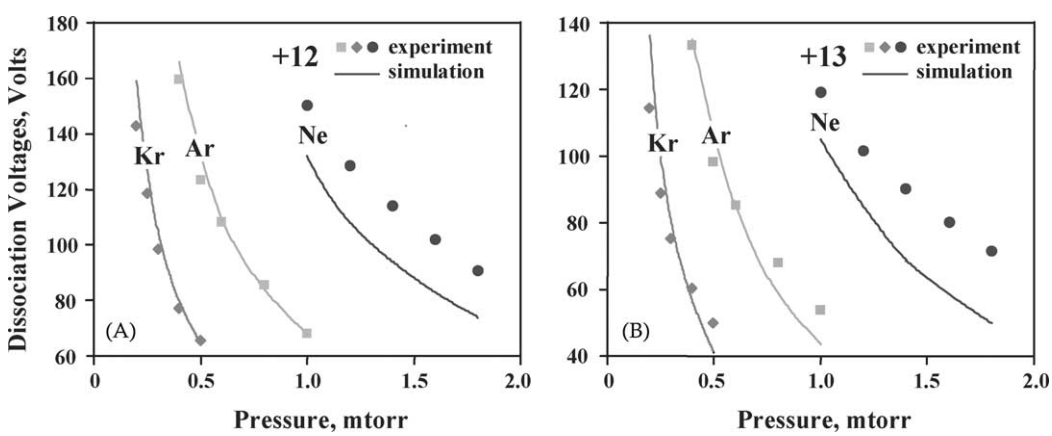

Fig. 6. Effect of the nature and the collision gas pressure on the dissociation of Trypsin–BPTI complex: (A) +12 charge state; (B) +13 charge state. Symbols represent experimental data, while solid lines correspond to simulation.

with Ne are obtained if the efficiency of the kinetic to internal energy conversion is reduced to ca. 87% as compared to 100% efficiency used for other gases.

The effect of the pressure of the collision gas on the dissociation voltages is also demonstrated in Fig. 6 and Table 1. Experimental data shows that dissociation voltages decrease with increase in pressure. Monte Carlo simulations closely reproduce experimental trends (Fig. 6A and B). It is interesting to note that both Monte Carlo and experimental results show a non-linear decrease in the halfway dissociation voltage with pressure. The non-linear dependence results from the gradual decrease in the ion kinetic energy as it passes through the collision cell and undergoes collisions. It follows that the rate of accumulation of the internal energy decreases with increase in the number of energizing collisions. In order to eliminate the effect of the mass of the collision gas on the dissociation voltage we decided to plot D_{50} as a function of the "reduced" pressure, given by the product of collision gas pressure and the ratio of the collision gas mass with that of Kr (Fig. 7). The results of Monte Carlo simulations for halfway dissociation voltages plotted in "reduced" coordinates (Fig. 7A) perfectly overlap with each other. This is not surprising, because the energy transfer efficiency in Monte Carlo simulations was assumed to be the same for all gases. Interestingly, there is a good overlap between the experimental results obtained for Ar and Kr in the reduced coordinates, indicating a similar energy transfer efficiency for these two gases (Fig. 7B). However, experimental values of D_{50} with Ne as a collision gas are higher than dissociation voltages obtained for heavier gases. This observation is in agreement with our earlier discussion on the lower energy transfer efficiency upon collisions of the Trypsin–BPTI complex with neon.

3.4.2.2. Comparison of experimental and simulated relative internal energies. The collision model results presented in Table 2 indicate that increase in the mass of the neutral target results in lowering of the values of RIE. For example, RIE required to dissociate both charge states of gas-phase Trypsin–BPTI complex ions during collisions with neutral gases shows a decrease in the order Ne > Ar at the pressure of 1 mTorr. Similar decrease in the order Ar > Kr was observed for RIE of these complexes at the pressure of 0.5 mTorr. Monte Carlo simulations conducted at the same pressure of different collision gases predict the same trend (Table 2). However, the absolute values of RIE obtained using the collision model and Monte Carlo simulations are quite different (Table 2). The collision model values of RIE for Ne are higher than simulated results, while the collision model RIE for collisions with Ar and Kr are lower and become close

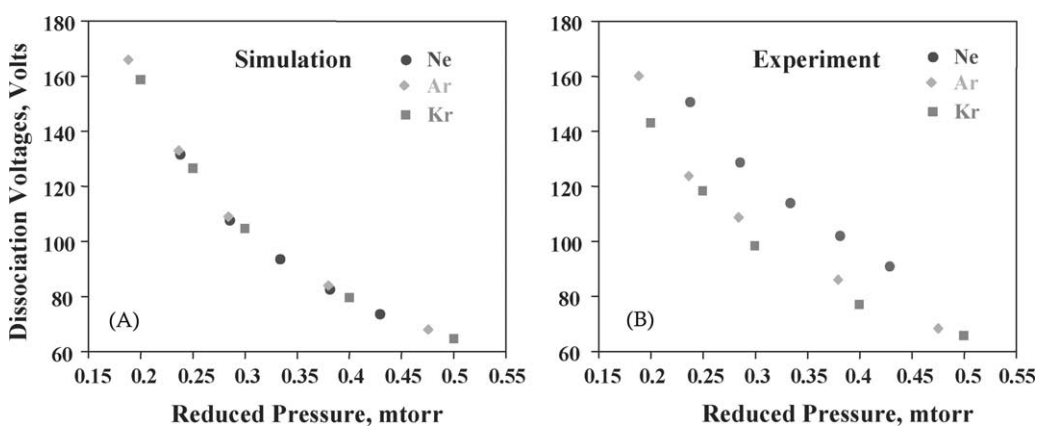

Fig. 7. Effect of the "reduced" pressure on the dissociation of +12 charge state of Trypsin–BPTI complex: (A) Monte Carlo simulation; (B) experimental observation.

to simulated results only at higher pressures. As discussed earlier we believe that the energy transfer efficiency in collisions with Ne is lower than for heavier collision gases. It follows that for Ne as collision gas both the collision model and the Monte Carlo simulation overestimate the amount of internal energy accumulated by the ion.

Monte Carlo simulations shows that increase in the pressure of the collision gas results in the decrease of relative internal energy required to induce 50% dissociation of the precursor ion (Table 2). The decrease in RIE as a function of pressure and mass of the collision gas is associated with the corresponding decrease in D_{50}, i.e., with the decrease in the initial ion kinetic energy. Motion of ions with lower kinetic energies through the collision cell is slower and the time available for reaction is longer. As a result, the average dissociation rate constant sampled in these experiments decreases with ion kinetic energy and the internal energy required for ion dissociation decreases correspondingly. Variation in reaction times as a function of different experimental parameters is shown in Table 1. Clearly, charge-state and pressure dependence of RIE are closely correlated with variations in the reaction time. Namely, somewhat lower RIE obtained for the +13 charge state result from longer time spent by the +13 charge state ions in the collision cell. Reaction time changes dramatically with pressure and the nature of the collision gas. For example, the two-fold increase in pressure (from 0.5 to 1 mTorr for Ar) is associated with an almost two-fold decrease in ion's kinetic energy required to observe 50% dissociation (from 1596 to 816 V, see Table 1) and proportional increase in the reaction time (from 67 to 102 μs). Following the increase in the reaction time (or the residence time in the collision cell) the RIE decreases from 132 to 122 eV (Table 2). The much smaller change in RIE results from the exponential dependence of the reaction rate constant on the internal energy.

However, this trend is not observed for the RIE obtained from the experimental data for the Trypsin–BPTI complex using the collision model. The results shown in Table 2 suggest that RIE does not change with pressure. It should be noted that decrease in RIE as a function of pressure has been observed previously for other protein complexes using the collision model treatment of dissociation voltages [25]. For example, increase in the pressure of the collision gas resulted in systematic decrease in relative internal energies required to dissociate cytochrome *c*-cytochrome b_5 complex [25].

The discrepancy between the pressure dependence of the RIE obtained from experimental data using the collision model and from Monte Carlo simulations can be rationalized based on the following considerations. Both models assume that ions move only along the axis of the quadrupole collision cell and there is no radial component of ions motion. However, it is well known that, in practice, this is not the case. The radial motion of the ion in the linear *rf* only quadrupole can be represented as a motion in an effective harmonic potential generated by the *rf* field [38]. However, the radial motion of the ion is efficiently damped by collisions with neutral gas. Collisional focusing characteristics of linear *rf* only quadrupoles have been widely utilized for improving ion transmission [22,23]. At sufficiently high pressures ion motion in a collisional quadrupole can be represented as a one-dimensional drift along the quadrupole axis, i.e., the kinetic energy of the ion has only the axial component. It follows that the collision model and Monte Carlo simulations presented in this work are best suited to represent ion motion in the collision cell at high pressures. At lower pressures the distance traveled by the ion inside the collision cell can be substantially larger than the cell length due to the radial motion of the ion. Consequently, RIE extracted from the low-pressure experimental data using the collision model are underestimated. In contrast, Monte Carlo simulations presented in this work were not utilized to obtain the best fit with experimental data but rather to predict the trends in RIE that should be obtained for a one-dimensional motion of ions through the collision cell. It follows that differences between the predictions of Monte Carlo simulations and the trends obtained from the experimental data using the collision model can be rationalized based on the above considerations.

3.5. Comparison of Monte Carlo simulations with theoretical computations

Monte Carlo simulations showed that it is possible to evaluate relative internal energy accumulated by precursor ion through a series of low-energy collisions with neutral gas. At the same time, calculation of relative internal energy is also possible through the use of previously derived theoretical expression from the collision model for an ion activation.

To compare results of Monte Carlo simulations with theoretical computations of relative internal energy, halfway dissociation voltage and its corresponding distance were extracted from the "computer" experiment and plugged into theoretical expression from the collision model for an ion activation. Following calculation of relative internal energies from theoretical expression and Monte Carlo simulations, their ratio was determined and used as measure of correlation between these two values. Monte Carlo simulations were repeated for both simple and diffuse scattering models for five incremental frequency factors ν from 10^6 to 10^{14}, five values of dissociation energies E_0 from 0.6 to 1.4 eV, and six numbers of effective oscillators s from 3000 to 8000. These simulation were conducted for four pressures (0.5, 1, 1.5, and 2 mTorr) of three different collision gases (Ne, Ar, and Kr).

Data presented in Table 3 shows that for simple model there is strong correlation between relative internal energies modeled by Monte Carlo simulation and those obtained from the theoretical expression derived from the collision model for an ion activation (Eq. (1)). Assessment of the correlation between relative internal energies obtained from Monte Carlo simulation and those calculated from the theoretical expression has been repeated with diffuse scattering model that included statistical distribution of the scattering angles, and the energies transferred to the ion. It was found that for a wide range of experimental parameters match of the internal energies of ions calculated from theoretical expression with those estimated by the Monte Carlo simulation was within about 6% (Table 3).

4. Conclusions

Monte Carlo simulations have been performed to model collisionally activated dissociation of the Trypsin–BPTI complex occurring in a collision cell of a triple quadrupole mass spectrometer. Application of collision dynamics to the statistically generated distances between collisions of precursor ion with neutral gas resulted in a comprehensive description of the precursor ion dissociation. Treatment of CAD as a stepwise process allowed to evaluate relative internal energy accumulated by the precursor ion after a series of low-energy collisions and determine dissociation rate constant using the RRKM expression. We have also shown that Monte Carlo simulations can be used to study the effect of the gradual unfolding of the precursor ion following a series of low-energy collisions on its fragmentation efficiency. Contrary to previous observations [25], it was found that simulation of the precursor ion dissociation depends on RRKM parameters and does not necessarily occur near the collision cell exit.

Table 3
Correlation of the relative internal energy calculated from the theoretical expression with those generated by Monte Carlo simulation

	Simple model			Diffuse model
	Ne	Ar	Kr	Kr
Points	209	296	367	368
Minimum	0.83	0.77	0.71	0.81
Maximum	1.14	1.18	1.18	1.14
Correlation	0.99 ± 0.06	1.00 ± 0.06	1.02 ± 0.06	0.98 ± 0.06

Monte Carlo simulation of the diffuse scattering collisions, that includes effects of scattering angle and energy transfer efficiency, produced results different from that obtained by a Monte Carlo simulation based on a simple collision model. Based on the data presented here it is difficult to evaluate which model better describes CAD process. Given the fact that dissociation voltages generated by both simple and diffuse Monte Carlo simulations were similar, smaller values of energy transfer efficiencies associated with diffuse Monte Carlo simulations would explain smaller values of RIE in comparison to simple Monte Carlo model. For both simple and diffuse scattering models relative internal energies obtained from Monte Carlo simulation showed a strong correlation with those calculated from the theoretical expression over a wide range of experimental parameters. Both simple and diffuse models can be used to reproduce experimental dissociation curves over a variety of experimental parameters. The major limitation of both the collision model and Monte Carlo simulations presented in this work is the assumption of a one-dimensional motion of the ion through the collision cell.

Further improvement in the performance of Monte Carlo simulation can be achieved by accurate modeling of the total distance traveled by the ion in the quadrupole field. Combination of Monte Carlo simulations presented with this work with recently published semi-quantitative [39] and computer models [28] predicting mean internal energy accumulated by ions in the electrospray interface region can provide a better theoretical description of ion dissociation in tandem mass spectrometry experiments.

Acknowledgements

This work was partially supported by the Genomics and Health Initiative from the National Research Council of Canada. Additional funding was jointly provided by the NSERC-SCIEX industrial chair, Office of Awards and Financial Aid and the Chemistry Department of the University of British Columbia. Part of this research was conducted under the auspices of the Office of Basic Energy Sciences, U.S. Department of Energy, under Contract DE-AC06-76RL0 1830 with the Battelle Memorial Institute, which operates the Pacific Northwest National Laboratory, a multi-program national laboratory operated from the Department of Energy.

References

[1] J.B. Fenn, M. Mann, C.K. Meng, S.F. Wong, C.M. Whitehouse, Science 246 (1989) 64.
[2] J.A. Loo, Mass Spectrom. Rev. 16 (1997) 1.
[3] Y.T. Li, Y.L. Hsieh, J.D. Henion, B. Ganem, J. Am. Soc. Mass Spectrom. 4 (1993) 631.
[4] M.J. Greig, H. Gaus, L.L. Cummins, H. Sasmor, R.H. Griffey, J. Am. Chem. Soc. 117 (1995) 10765.
[5] K.A. Sannes-Lowry, H.-Y. Mei, J.A. Loo, Int. J. Mass Spectrom. 193 (1999) 115.
[6] T.J.D. Jorgensen, T. Staroske, P. Roepstorff, D.H. Williams, A.J.R. Heck, J. Chem. Soc., Perkin Trans. 2 (1999) 1859.
[7] J.A. Loo, P. Hu, P. McConnell, W.T. Mueller, T.K. Sawyer, V. Thanabal, J. Am. Soc. Mass Spectrom. 8 (1997) 234.
[8] Y.T. Li, Y.L. Hsieh, J.D. Henion, T.D. Ocain, G.A. Schiehser, B. Ganem, J. Am. Chem. Soc. 116 (1994) 7487.
[9] D.S. Gross, Y. Zhao, E.R. Williams, J. Am. Soc. Mass Spectrom. 8 (1997) 519.
[10] D.J. Butcher, K.G. Asano, D.E. Goeringer, S.A. McLuckey, J. Phys. Chem. 103 (1999) 8664.
[11] H. Rogniaux, A. Van Dorsselaer, P. Barth, J.F. Biellmann, J. Barbanton, M. van Zadt, B. Chevrier, E. Howard, A. Mitschler, N. Potier, L. Urzumtseva, D. Moras, A. Podjarny, J. Am. Soc. Mass Spectrom. 10 (1999) 635.
[12] T.J.D. Jørgensen, D. Delforge, J. Remacle, G. Bojesen, P. Roepstorff, Int. J. Mass Spectrom. Ion Process. 118 (1999) 63.
[13] C.L. Hunter, A.G. Mauk, D.J. Douglas, Biochemistry 36 (1997) 1018.
[14] R.N. Hayes, M.L. Gross, Methods Enzymol. 193 (1990) 237.
[15] A.K. Shukla, J.H. Futrell, Mass Spectrom. Rev. 12 (1993) 211.
[16] T. Baer, W.L. Hase, Unimolecular Reaction Dynamics: Theory and Experiments, Oxford University Press, New York, 1996.
[17] K.A. Holbrook, M.J. Pilling, S.H. Robertson, Unimolecular Reactions, Wiley, New York, 1996.
[18] J. Laskin, M. Byrd, J.H. Futrell, Int. J. Mass Spectrom. 195/196 (2000) 285.
[19] J. Laskin, J.H. Futrell, J. Phys. Chem. A 104 (2000) 5484.
[20] J. Laskin, E. Denisov, J.H. Futrell, J. Am. Chem. Soc. 122 (2000) 9703.
[21] J. Laskin, J.H. Futrell, J. Chem. Phys. 116 (2002) 4302.
[22] D.J. Douglas, J. Am. Soc. Mass Spectrom. 9 (1998) 101.
[23] D.J. Douglas, J.B. French, J. Am. Soc. Mass Spectrom. 3 (1992) 398.

[24] V.J. Nesatyy, J. Mass Spectrom. 36 (2001) 950.
[25] M.R. Mauk, A.G. Mauk, Y.-L. Chen, D.J. Douglas, J. Am. Soc. Mass Spectrom. 13 (2002) 59.
[26] Y.-L. Chen, J.M. Campbell, B.A. Collings, L. Konermann, D.J. Douglas, Rapid Commun. Mass Spectrom. 12 (1998) 1003.
[27] M. Fujiwara, Y. Naito, Rapid Commun. Mass Spectrom. 13 (1999) 1633.
[28] A. Hoxha, C. Collette, E. De Pauw, B. Leyh, J. Phys. Chem. A 105 (2001) 7326.
[29] H.R. Skullerud, J. Phys. Chem. B: Atom. Mol. Phys. 6 (1973) 728.
[30] P.S. Epstein, Phys. Rev. 23 (1924) 710.
[31] J.R. Stalder, V.J. Zurick, National Advisory Committee for Aeronautics TN 2423, NACA, 1951.
[32] Y.-L. Chen, B.A. Collings, D.J. Douglas, J. Am. Soc. Mass Spectrom. 8 (1997) 681.
[33] V. Nesatiy, Y.-L. Chen, B.A. Callings, D.J. Douglas, Rapid Commun. Mass Spectrom. 12 (1998) 40.
[34] M. Meroueh, W.L. Hase, Int. J. Mass Spectrom. 201 (2000) 233.
[35] E.M. Marzuff, S.A. Campbell, M.T. Rodgers, J.L. Beauchamp, J. Am. Chem. Soc. 116 (1994) 6947.
[36] K.B. Shelimov, M.F. Jarrold, J. Am. Chem. Soc. 118 (1996) 10313.
[37] K.B. Shelimov, D.E. Clemmer, R.R. Hudgins, M.F. Jarrold, J. Am. Chem. Soc. 119 (1997) 2240.
[38] P.H. Dawson (Ed.), Quadrupole Mass Spectrometry and Its Applications, Springer, New York, 1995.
[39] B.B. Schneider, D.D.Y. Chen, Anal. Chem. 72 (2000) 791.